Journal of Applied Polymer Science

Improved Conductivity and Thermal Stability by the Formation of a Charge-Transfer Complex in β-Nucleation-Agent-Nucleated and MWCNT-Filled iPP Composites

Yu Zhang, Hong Liu, Lei Zhang, Xinpeng Li, Hainan Du, Jie Zhang

State Key Laboratory of Polymer Materials Engineering, College of Polymer Science and Engineering, Sichuan University, Chengdu, People's Republic of China

Correspondence to: J. Zhang (E-mail: zhangjie@scu.edu.cn)

ABSTRACT: In this study, the influence of β-nucleation agent (β-NA) on the morphology and properties of multi-walled carbon nanotube (MWCNT) filled isotactic polypropylene (iPP) composites was explored in details. The results show that the incorporation of β-NA has promoted the dispersion of MWCNT in the iPP matrix, which is profitable for improving the thermal stability and conductivity properties of MWCNT-iPP composites. Besides, the 0.05 wt % β-NA nucleated samples exhibit higher impact toughness than that of un-β-NA-nucleated ones. Further SEM observations show that the morphology of MWCNT changes from large agglomerations to small clusters with doping of β-NA. The main reason is that the incorporation of β-NA (TMB-5) in MWCNT filled iPP matrix has led to the formation of a charge-transfer complex. Some of these clusters act as nucleation sites for inducing crystallization of α spherulites, which have a compete growth with β-NA induced β crystals. Meanwhile, other clusters exist in the inter-lamella amorphous phase of β crystals, some of them even combine two adjacent β spherulites. Accordingly, a large conductive network comes into being. Based on the investigated results, a mechanism model is proposed. © 2013 Wiley Periodicals, Inc. J. Appl. Polym. Sci. 000: 000–000, 2013

KEYWORDS: conducting polymers; composites; polyolefins; nanotubes; graphene and fullerenes; morphology

Received 23 November 2012; accepted 28 December 2012; published online
DOI: 10.1002/app.38987

INTRODUCTION

Since the landmark paper by Iijima in 1991,[1] carbon nanotubes (CNT) have generated huge activity in many areas of science and engineering due to their very large aspect ratio, extraordinary electrical, mechanical, and thermal properties. In polymer research field, the first polymer nanocomposites using CNT as a filler were reported by Ajayan et al. in 1994.[2] After that, large amounts of literatures[3–10] about the improved performances of polymer materials by the addition of CNT were reported.

Codek et al.[3] studied mechanical and thermal properties of amorphous and crystalline polymers with multi-walled carbon nanotube (MWCNT) and observed significant improvement in their properties. Long and Chen[4] reported that an ultrahigh electrical conductivity of 100 S/m was achieved for a polymer composite consisting of 25 mass% randomly oriented nanotubes in polyaniline. Xiao et al.[5] found that Young's modulus and tensile strength of low density polyethylene increased by 89% and 56%, when the nanotube loading reached 10 wt %.

In spite of this, CNT often aggregate due to high van der waals forces and physical entanglements, and the efficiency of CNT to improve the composites properties depends on dispersion of CNT within the matrix materials. In recent years, researchers have used many different techniques to attempt an efficient dispersion of nanotubes in polymer matrices, including fictionalization of CNT surface,[11–16] use of polymers to coat the nanotube surface,[17] *in situ* polymerization,[18,19] ultrasonic dispersion in solution or suspension,[20–22] electrospinning,[23] use of surfactants.[16,24]

Although these modification methods are highly active in improving the dispersion of CNT, they are too complicated for practical manufacturing and application, even some of them would destroy the intrinsic structure of CNT. Thus, exploring a convenient and feasible technique to disperse CNT well in the polymer matrix is a promising study area. In the present work, we prepared β-NA-nucleated MWCNT-filled composites by melt compounding method, to investigate the influence of β-NA on the MWCNT in isotactic polypropylene (iPP) matrix and found that the β-NA has a promoting dispersion effect on the dispersing of MWCNT, which is advantageous for improving the conductivity and thermal stability of composites simultaneously. Based on the investigated results, a model for

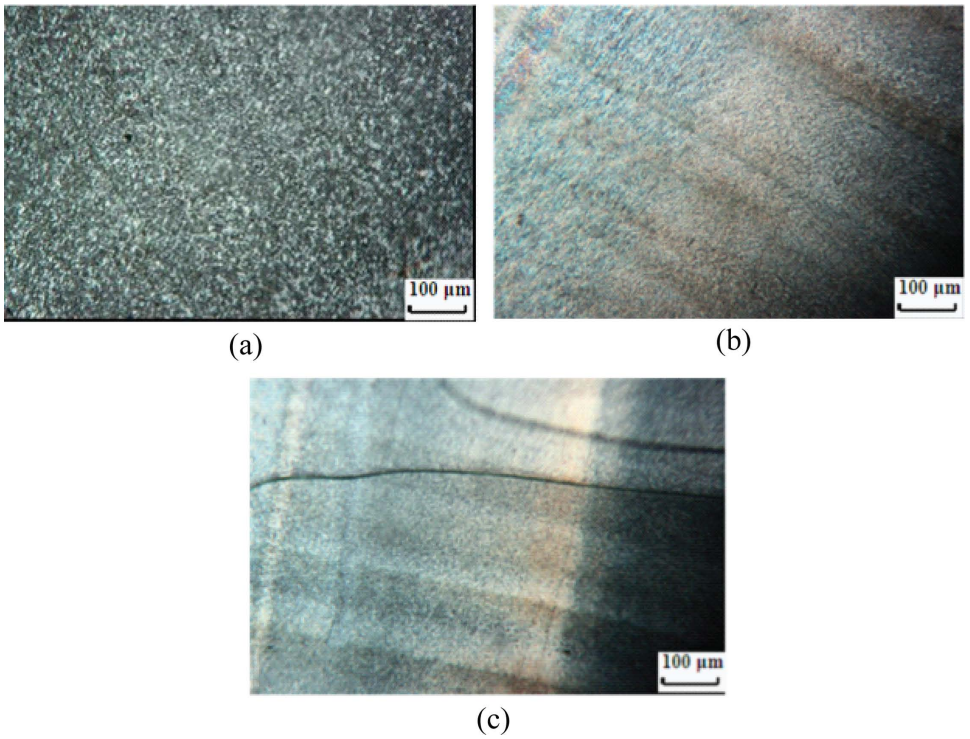

Figure 1. PLM images of core layer of (a) iPP/0-0, (b) iPP/0.05-0, and (c) iPP/0.2-0, respectively, reflecting the change of spherulites size after the addition of β-NA. [Color figure can be viewed in the online issue, which is available at wileyonlinelibrary.com.]

explaining the mechanism concerning conductivity improvement by the incorporation of β-NA in MWCNT-filled samples is proposed.

EXPERIMENT SECTION

Materials

The iPP (trade name T30S) used in this study was purchased from Lanzhou Petrochemical Company, China, with a melt flow index (MFI) of 2.6 g/10 min (230°C/2.16 kg) and a density of 0.91 g/cm^3, respectively. The TMB-5 β-nucleation agent (β-NA) is aryl amide compound, which has a similar chemical structure as some aromatic amine β-phase NA, such as N,N′-dicyclohexyl-2,6-naphthalenedicarboxamide. This compound was obtained from Shanxi Provincial Institute of Chemical Industry. MWCNT grown by catalytic chemical vapor deposition were supplied by Nanocyl SA (Belgium), with an average diameter of 9.5 nm, length of 1.5 μm, and 90% carbon purity (10% metal oxide) according to the manufacturer's specification. In this study, the MWCNT were used without any other pretreatment.

The β-NA contents chosen in this study are 0.05 and 0.2 wt %. They are selected because the former content is proved to be the critical content (0.03–0.05 wt %) to achieve well-developed

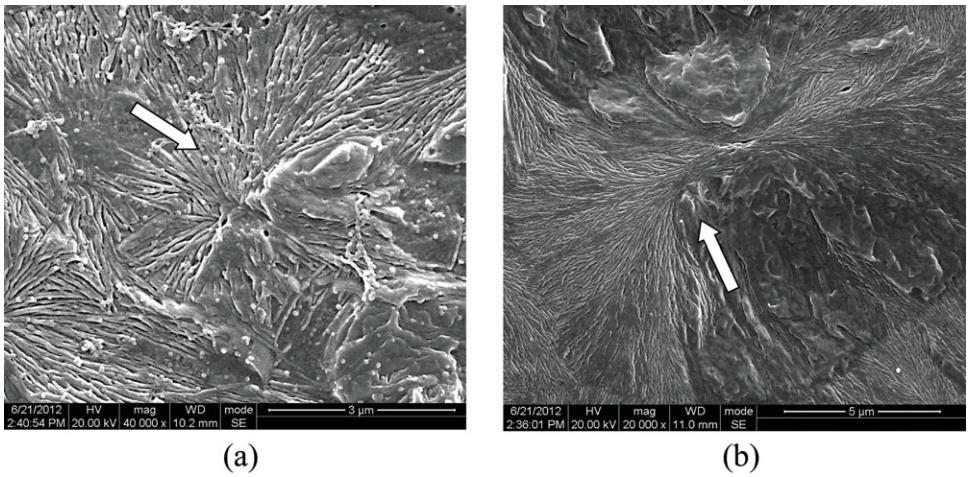

Figure 2. SEM images of supermolecular structure of (a) iPP/0.05-0, (b) iPP/0.2-0, respectively. The arrows are pointing at β spherulites.

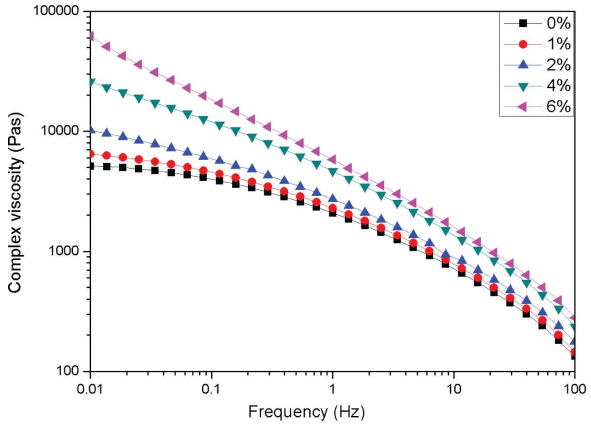

Figure 3. Effect of MWCNT contents on the complex viscosity of iPP. [Color figure can be viewed in the online issue, which is available at wileyonlinelibrary.com.]

β spherulites, and the latter is the supercritical one for iPP[25,26] (for convenience, iPP with 0.05 wt % TMB-5 and 0.2 wt % TMB-5, shown as iPP/0.05 and iPP/0.2, respectively). The iPP pellets without β-NA were also prepared under the same processing conditions for comparison purpose (designated as iPP/0). The MWCNT were added to β-nucleated and non-β-nucleated iPP at concentrations of 1, 2, 4, and 6%. Here, the number after the notation of each sample represents its corresponding MWCNT concentration. For example, iPP/0.05-4 stands for the sample of iPP with 0.05 wt % TMB-5 and 4 wt % MWCNT, while iPP/0.2-0 represents the sample of iPP with 0.2 wt % TMB-5 and no additive MWCNT.

Sample Preparation

To achieve a good dispersion of β-NA in iPP, a two-step process was employed to prepare the materials. Namely, TMB-5 was first melt mixed with iPP to form master batch containing 5 wt% β-NA. The master batch was then further compounded with pure iPP and MWCNT using a SHJ-25 twin-screw extruder. The screw speed was fixed at 120 rpm, and the processing temperature profile was limited within 170–220°C from hopper to die.

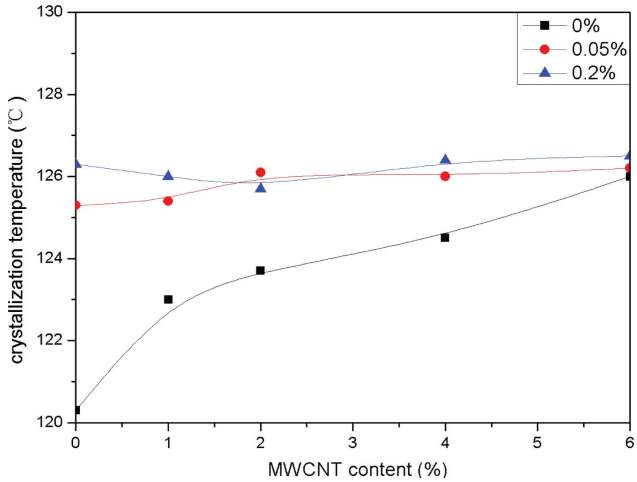

Figure 4. Crystallization temperature of composites of various β-NA contents and MWCNT contents. [Color figure can be viewed in the online issue, which is available at wileyonlinelibrary.com.]

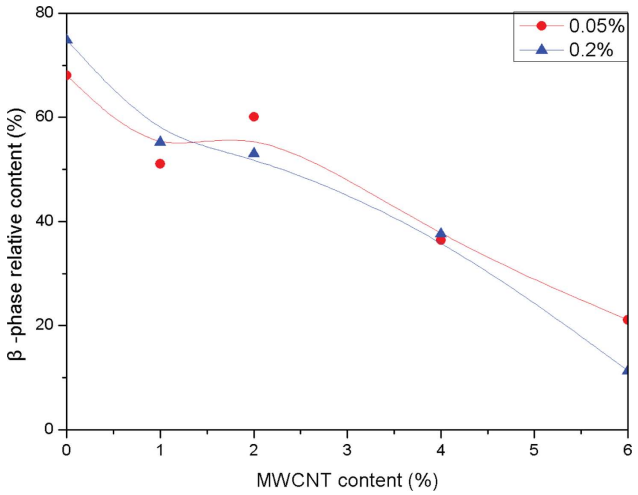

Figure 5. Relative content of β-phase (K_β) of β-NA nucleated samples with addition of MWCNT. [Color figure can be viewed in the online issue, which is available at wileyonlinelibrary.com.]

Rectangular parallelopiped shape samples (125 × 13× 4 mm) were prepared by means of a PS40E5ASE injection molding machine with a barrel temperature of 220°C, mold temperature of 60°C and injection pressure of 35 MPa.

For preparing dynamic rheology tests, the mixed pellets were compression molded into specific disks (1.2 mm thick with a diameter of 25 mm) at 200°C for 5 min. The applied pressure was 10 kN. The force was released to zero twice in order to allow any potential gas to escape.

Characterization

PLM Observations. Thin slices cut by means of a microtome were used for optical morphology observations. The sampling zones were located in the middle of samples along the flow direction. Morphology observations were conducted using DX-1 (Jiang Xi Phoenix Optical Co., China) microscope connected to a Nikon 500D digital camera.

Dynamic Rheology Measurements. Dynamic rheology properties were investigated using a rotational rheometer (Malvern Instruments, Bohlin Gemini 200). Steady shear measurement was performed at the shear rate of 0.01–100 s^{-1} at 200°C.

DSC Tests. The crystallization and melting behaviors of the samples were carried out on a TA Q200 differential scanning calorimeter in a nitrogen atmosphere. A sample about 8 mg was first heated up to 200°C and held on for 5 min to release thermal history. Then, it was cooled down to 40°C at a cooling rate of 10°C/min to investigate the crystallization behavior of the sample. After maintaining at 40°C for 1 min, it was heated up again to 200°C at 10°C/min to explore the melting behavior of the sample.

The fusion enthalpy (ΔH_i) of α crystal and β crystals was obtained by the methods proposed by Li,[27] and the

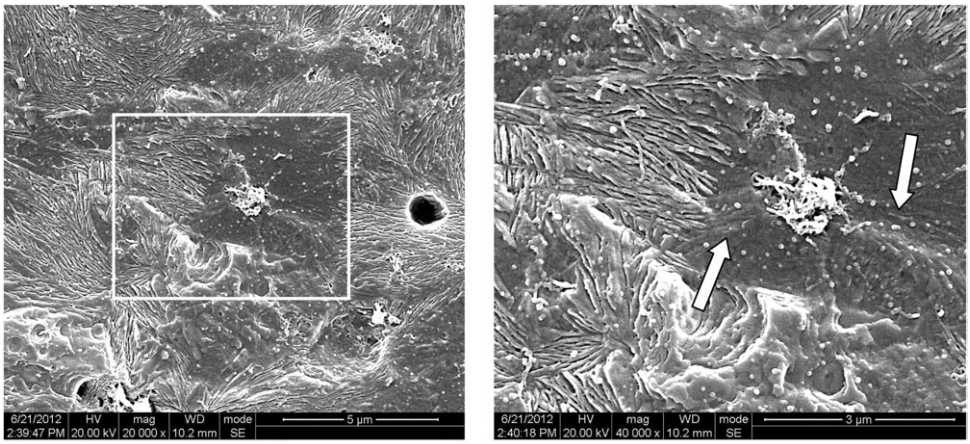

Figure 6. SEM photographs of competition growth between MWCNT nucleated α crystals and β-NA nucleated β crystals. The image (b) corresponds to the part in the white box of the image (a). The white arrows in image (b) point to some α lamellas grown from MWCNT clusters.

crystallinities of the α- and β-phase were calculated separately according to equation:

$$X_i = \Delta H_i/(\Delta H_i^0 \times \Phi_c) \times 100\% \quad (1)$$

Where ΔH_i is the calibrated specific fusion heat of either the α-phase or the β-phase and ΔH_i^0 is the standard fusion heat of either α-phase or the β-phase crystals, 178 J/g for the former and 170 J/g for the latter, and Φ_c is the weight percentage of iPP in composites.

The relative fraction of β-phase (K_β) in the matrix can be calculated from the following equation:

$$K_\beta = \frac{X_{c\beta}(\%)}{X_{c\alpha}(\%) + X_{c\beta}(\%)} \times 100\% \quad (2)$$

where $X_{c\alpha}$ (%) and $X_{c\beta}$ (%) are the degrees of crystallinity for α-phase and β-phase, respectively.

Izod Impact Strength Test. The notched Izod impact strength was used to evaluate the toughness of the samples. The notched specimens were tested with a VJ-40 impact test machine at room temperature, according to GB/T 1843-2008 standard. Each impact test was repeated at least eight times, and the results were averaged.

TGA Tests. Thermal degradation was measured on approx. 10 mg sample in a NETZSCH TG 209F1 Iris system, with alumina pan in a 100 cm^3/min nitrogen flow and with a 10°C/min heating ramp from room temperature up to 750°C. Thermo-oxidation was determined in the same way in a 100 cm^3/min air flow and with a 10°C/min heating ramp from room temperature up to 750°C.

The "thermal stability temperature" T_s which is defined in this paper corresponds to the temperature at which the weight loss of composites is 90%, which is a reflection of thermal stability.

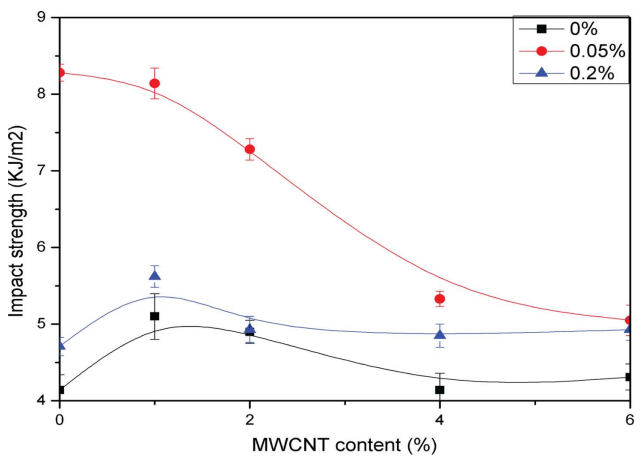

Figure 7. Izod notched impact strength of β-NA nucleated and MWCNT-filled iPP. [Color figure can be viewed in the online issue, which is available at wileyonlinelibrary.com.]

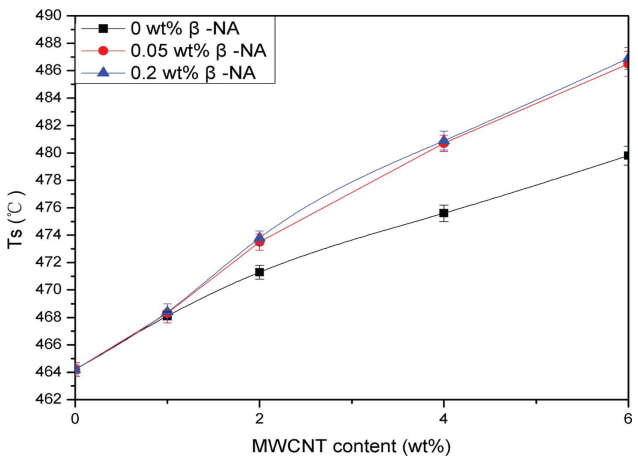

Figure 8. Effect of β-NA on the "thermal stability temperature" T_s in nitrogen atmosphere. [Color figure can be viewed in the online issue, which is available at wileyonlinelibrary.com.]

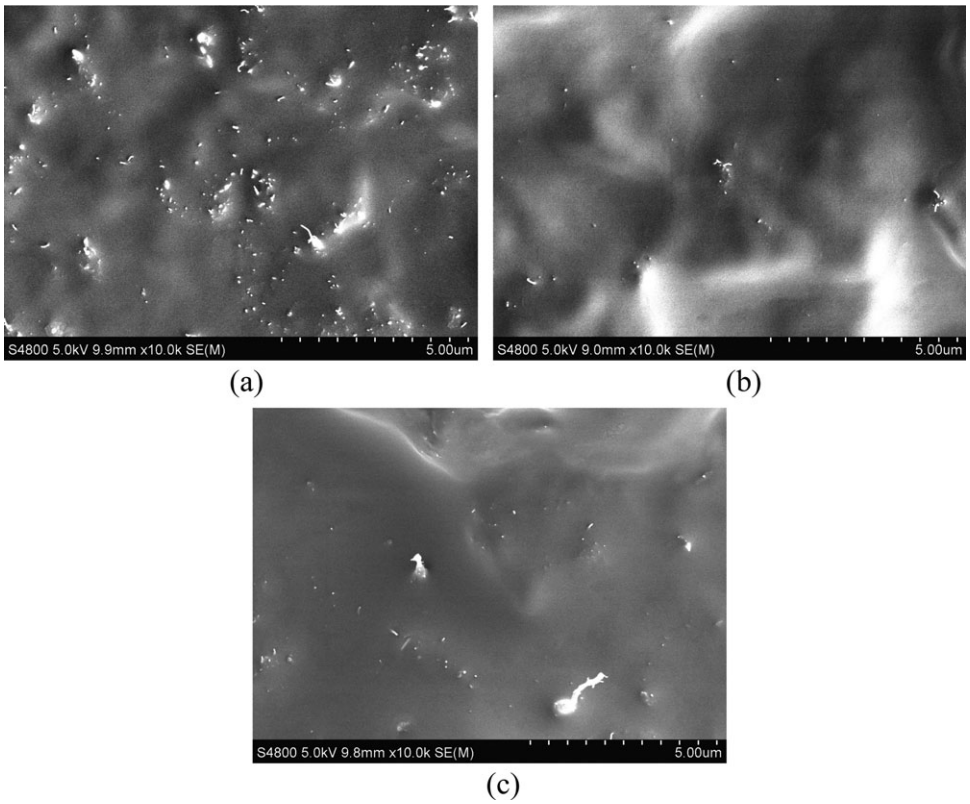

Figure 9. SEM images of cryo-fractured surfaces of core layer of (a) iPP/0-6, (b) iPP/0.05-6, and (c) iPP/0.2-6, respectively.

Each measurement was repeated at least for three times, and the T_s values were averaged.

SEM Observations. In order to investigate the dispersion of MWCNT in the matrix, specimens cut from the center of the sample were fractured in liquid nitrogen, and the cryo-fractured surfaces of the composites were observed using a Hitachi scanning electron microscope (Model S4800; Hitachi, Osaka, Japan).

A Konics field emission scanning electron microscope (model KYKY2800, China) was used for examining morphology variation of iPP crystalline phase with the doping of β-NA as well as its influence on the MWCNT dispersing, samples were etched at 100°C for 6 min. Prior to microscopic examination, the surfaces of the specimens were coated with a thin layer of gold by ion sputtering.

Electrical Properties Measurements. DC measurements were performed at room temperature on specimens cut from the middle of samples prepared by injection molding. The electrical conductivity achieved by the measurements in this study refers to the flow direction of the specimens, having a cross-section dimension of 13 × 4 mm, and the longitudinal direction is 10 mm. Both ends of the specimens were coated with conductive silver paint. The electrical conductivity σ was then calculated according to:

$$\sigma = L/RA \tag{3}$$

where L is the distance between the electrodes, A is the cross sectional area, and R is the measured resistance. The characterization of high resistivity specimens was conducted using a high resistance meter (Keithley 6517A), while the low resistivity specimens were tested using a Keithley 6487 source meter.

RESULTS AND DISCUSSION

Influence of β-NA on the Morphology of iPP

Figure 1 shows the optical microscopy of non-nucleated and β-NA nucleated polypropylene samples without MWCNT. From Figure 1(a), large amounts of spherulites (Maltese cross), even though a little small, can be clearly seen. However, with the addition of β-NA, the spherulites size decreases dramatically so that no clear Maltese cross can be seen any more, as shown in Figure 1(b,c). It indicates that the β-NA act as nucleation sites for crystallization.

Figure 2 exhibits the supermolecular structure of β-NA nucleated samples in the absence of MWCNT. The critically nucleated sample (iPP/0.05-0) presents well-developed β-spherulites structure, while the supercritically nucleated sample displays bundle-like morphology without distinctly developed spherulites, which corresponds to the observations of Kotek et al.[25,26]

Influence of MWCNT on the Rheology Properties of iPP

The effect of MWCNT contents on the complex viscosity of iPP samples is shown in Figure 3. It can be seen that MWCNT-filled iPP exhibit higher complex viscosity than neat iPP at whole frequency ranges (10^{-2}–10^{2} Hz), indicating confinement of iPP chains with the addition of MWCNT.[28] Frequency thinning effect can be detected for all samples, and the viscosity

Applied Polymer SCIENCE

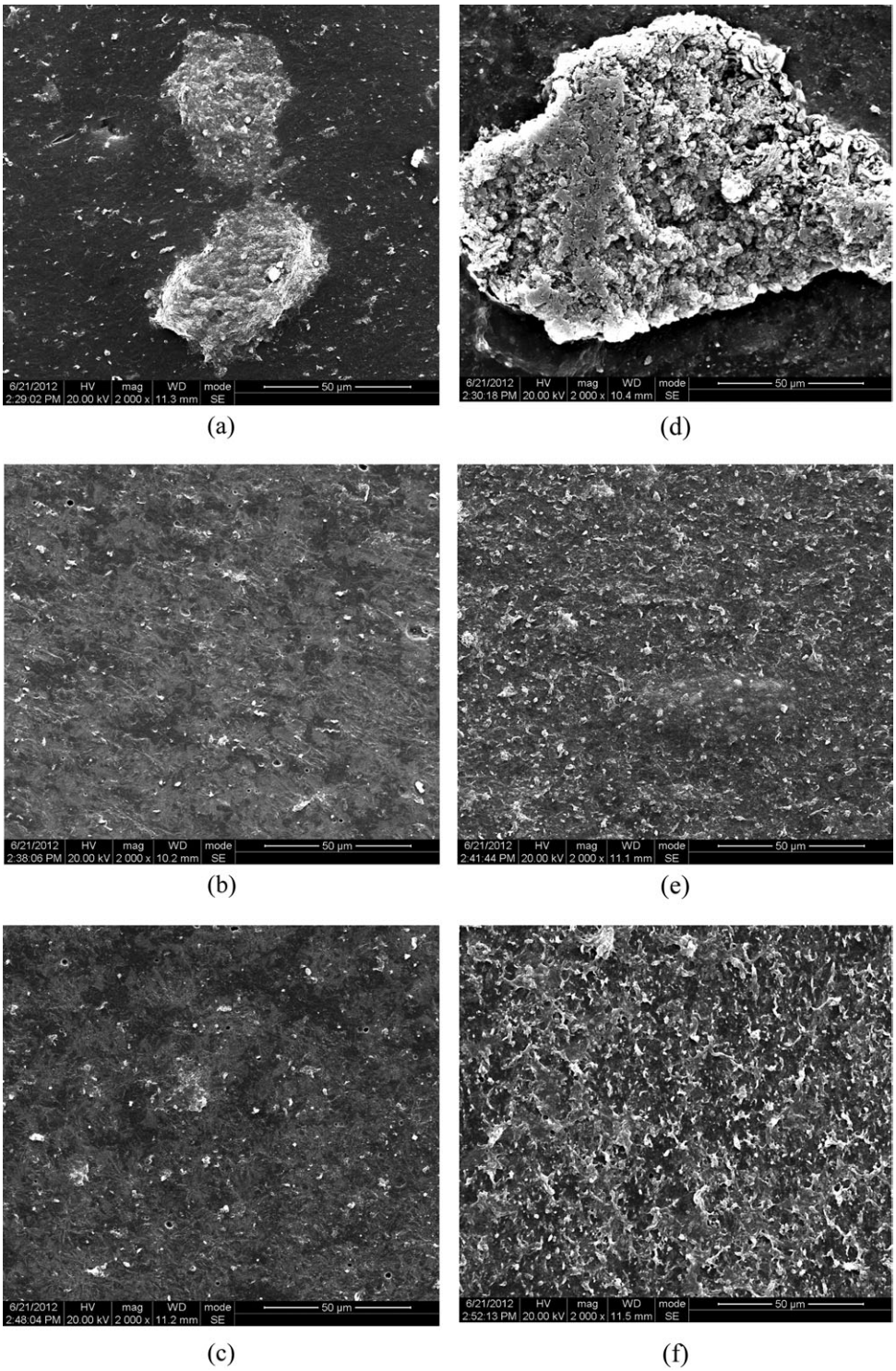

Figure 10. SEM images of etched surfaces of core layer of (a) iPP/0-2, (b) iPP/0.05-2, (c) iPP/0.2-2, (d) iPP/0-6, (e) iPP/0.05-6, and (f) iPP/0.2-6, respectively.

difference by the doping of MWCNT in iPP is not obvious at high frequency.

Properties

Figure 4 depicts the crystallization temperature of composites of various β-NA contents and MWCNT contents. It can be seen that the incorporation of MWCNT increases the crystallization temperature of iPP, indicating that MWCNT act as nucleation agent for crystallization. Taking into account that there is no β melting peak for MWCNT-filled samples (not shown here), it can be deduced that MWCNT is a kind of α nucleation agents, which corresponds to the results of some other researchers.[29–32]

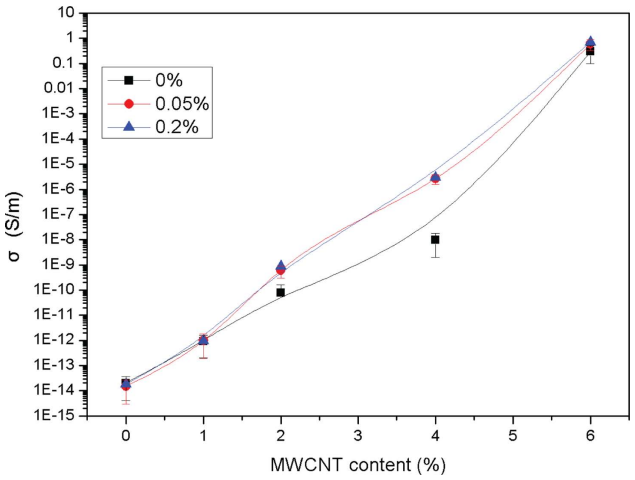

Figure 11. DC conductivity of non-β-NA nucleated and β-NA nucleated composites samples as a function of MWCNT concentration (wt %). [Color figure can be viewed in the online issue, which is available at wileyonlinelibrary.com.]

Comparatively, the crystallization temperature of β-NA nucleated samples keeps nearly unchanged with the incorporation of MWCNT. The main reason is that the addition of β-NA has improved the crystallization temperature to a high level, thus the influence of further additive MWCNT is little.

Figure 5 shows the relative content of β-phase in the β-NA nucleated samples. It can be clearly seen that the K_β decreases gradually with the addition of MWCNT.

Based on these results, it can be speculated that there may exist a competition growth between MWCNT nucleated α crystals and β-NA nucleated β crystals. Figure 6 presents SEM images of β-NA-nucleated MWCNT-filled samples after being etched, which confirms the speculation. A MWCNT-nucleated α spherulite is surrounded by several β spherulites, and the lamellas of α and β crystals form a rough interface, indicating that MWCNT induced α crystals have a crystal growth competition with β-NA induced β crystals in iPP matrix.

Figure 7 depicts the notched impact strength of β-NA nucleated and MWCNT-filled iPP. It can be viewed that the 0.05 wt % β-NA nucleated samples exhibit the superior toughness compared with 0.2 wt % β-NA nucleated and non-nucleated samples. Although the relative fraction of β crystals are almost the same in 0.05 wt % and 0.2 wt % β-NA nucleated samples, the impact strength of the latter is lower than that of former (more obvious at low MWCNT content range). The main reason is that the β spherulites of 0.2 wt % β-NA nucleated samples are bundle-like rather than well developed.[26] However, with the addition of MWCNT, this superiority was weakened. On one hand, the doping of MWCNT destroys the structure perfection of β spherulites; on the other hand, the aggregated MWCNT act as stress concentration points in the samples, which are detrimental to toughness of composites.

Figure 8 shows the effect of β-NA on the half weight loss temperature in nitrogen atmosphere, indicating that the incorporation of β-NA improves the thermal stability of composites when MWCNT content is beyond 1 wt %. In Zanetii's study, it has been shown that the degree of MWCNT dispersion is related to the thermal stability of composites.[33] It can be expected that the dispersion degree of MWCNT changes with the addition of β-NA, thus in order to confirm the deduction, detailed SEM observations were conducted.

Improved Dispersion of MWCNT by the Incorporation of β-NA

Figure 9 depicts the cryo-fractured surfaces of core layer of 6 wt % MWCNT filled samples with various contents of β-NA. It can be seen from Figure 9(a) that there exist some MWCNT agglomerations in cryo-fractured surface of iPP/0-6, but the incorporation of β-NA has lowered the degree of aggregating dramatically.

In order to better investigate the promoting effect caused by the addition of β-NA, the etched surfaces were also observed, as

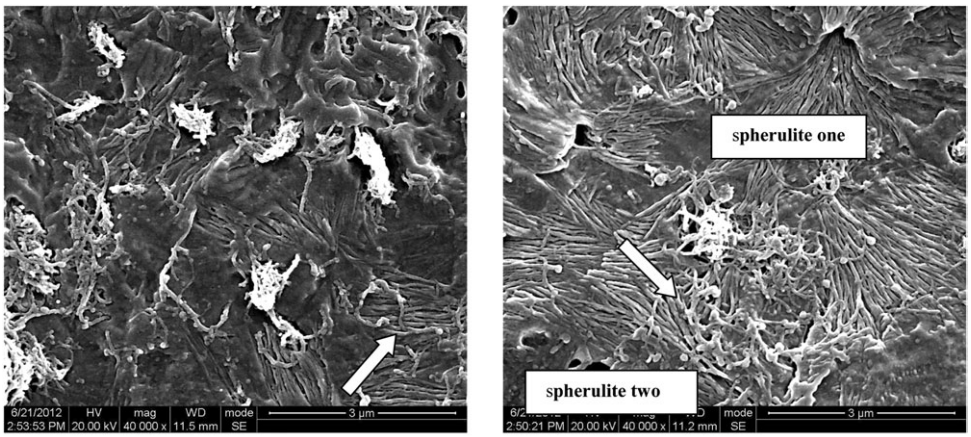

Figure 12. SEM images reflecting the distribution of MWCNT clusters in β crystals. The left graph is taken from iPP/0.2-2, and the right one is from iPP/0.2-6. The arrows are indicating the distribution of MWCNT clusters among the β spherulites.

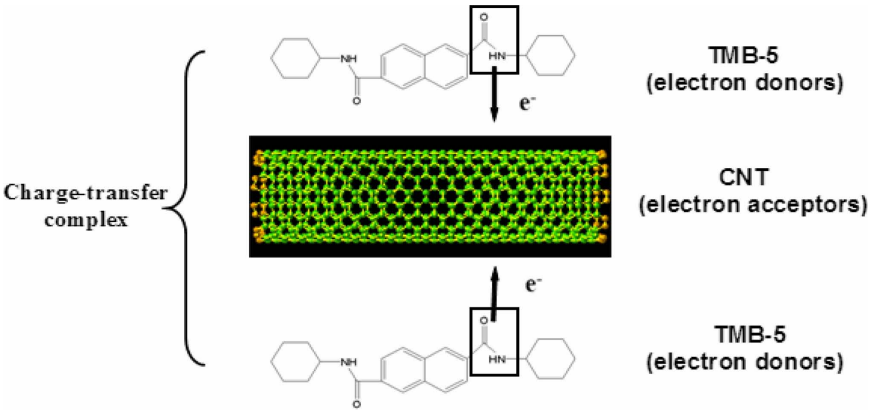

Figure 13. Schematic illustration of interaction between TMB-5 and CNT in iPP matrix. [Color figure can be viewed in the online issue, which is available at wileyonlinelibrary.com.]

shown in Figure 10. In Figure 10(a,d), MWCNT agglomerations with large size can be found in the matrix for the reason that MWCNT have an intensive tendency to aggregate. However, with the addition of β-NA, no agglomerations as obvious as that of non-β-NA-nucleated sample can be observed. It confirms that the addition of β-NA has a "promoting dispersion effect" on the dispersing of MWCNT. Therefore, relatively well-dispersed MWCNT result from the doping of β-NA accounts for the improved thermal stability of composites, and this effect is more pronounced when the MWCNT content is beyond 1 wt % (Figure 8). The possible reason is that when the MWCNT content is low (below 1 wt %), the promoting dispersion effect is not obvious.

Improved Conductivity of Composites by the Incorporation of β-NA

Figure 11 presents the DC conductivity of non-β-NA nucleated and β-NA nucleated composites as a function of MWCNT concentration. There is no obvious difference between non-β-NA nucleated and β-NA nucleated composites when the MWCNT concentration is below 1 wt %, which is similar to the results of TGA. At the 1–6 wt % MWCNT concentration range, the conductivity was improved evidently by the addition of β-NA for the reason that β-NA can disperse MWCNT much well, which is advantageous for the improvement of conductivity. It is expected that the incorporation of β-NA has lowered conductive percolation threshold than that of non-β-NA nucleated samples The conductive percolation threshold changes from 4.5% (non-β-NA nucleated) to 3.1% (0.05%-β-NA nucleated) or 3.0% (0.2%-β-NA nucleated) with the addition of β-NA. At 6 wt % MWCNT content, the conductivity divergence is little due to the fact that the conductive network has formed at high MWCNT concentration, so the influence of β-NA can be ignored. Besides, there is little diversity of conductivity between 0.05 and 0.2 wt % β-NA nucleated samples (the difference of percolation threshold is only 0.1%), indicating that the

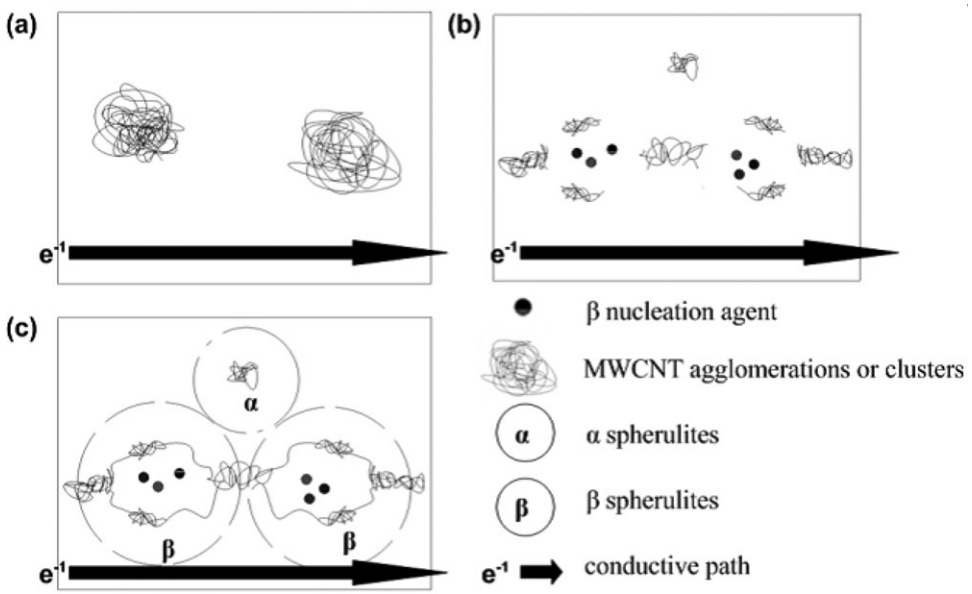

Figure 14. The schematic drawing of the morphology evolution of MWCNT-filled sample after the incorporation of β-NA.

supercritical content of β-NA has similar influence on the dispersion of MWCNT to that of critical content.

Distribution of MWCNT Clusters in β Crystals

Since the addition of β-NA has promoted the dispersion of MWCNT and improved the conductivity of MWCNT-filled composites, the investigation about the distribution of MWCNT clusters in β-NA induced β crystals is meaningful. It can be seen from Figure 12(a) that a single MWCNT goes across the lamellas of β crystals (hinted by the white arrow), indicating that MWCNT can disperse in the inter-lamella amorphous phase of crystallites. The main reason is that the lamellas of crystals are compact, thus the MWCNT will reject from the crystallites and can only reside in the amorphous region.[34] Figure 12(b) shows that there exist a few MWCNT clusters can go through two neighboring β crystals, and they act as a tie linking two distinct β spherulites. The reason is that MWCNT have a large aspect ratio, even if in the form of clusters. One β crystal is not big enough to hold these clusters, thus they will distribute in distinct β crystals.

Mechanism Model

Figure 13 presents the schematic illustration of interaction between TMB-5 and CNT in iPP matrix. It has been established that CNT are natural electron acceptors.[35] Meanwhile, the amide groups of TMB-5 chains are electron donors. Thus, the free amine groups of TMB-5 chains can interact with the surface of CNT and get absorbed through the formation of a charge-transfer complex.[36,37] As a result, the Van der waals forces between CNT are weakened, the morphology of MWCNT changes from large agglomerations to small well distributed clusters with doping of β-NA (Figure 14).

MWCNT chains are entangled as large agglomerations in the iPP matrix in the absence of β-NA [Figure 14(a)]. After the incorporation of β-NA, the morphology changes obviously. During the melt compounding process, the small β-NA molecules are immersed into the MWCNT agglomerations and led to the formation of a charge-transfer complex, influencing the van der waals forces of MWCNT agglomerations, and the intensive shear force imposed in the melt compounding process further destroy these agglomerations. Therefore, the dispersion of MWCNT is highly improved. As a result, the agglomerations are divided into separated clusters, as depicted in Figure 14(b). It has been proposed by Cardoso that the presence of well distributed clusters, rather than a fine dispersion, is more important for achieving larger conductivity for a given CNT concentration,[38] so these well dispersed clusters after the incorporation of β-NA account for the improvement of conductivity. Figure 14(c) shows the morphology of composites after the crystallization. The β-NA can induce the formation of β crystals, which encircle some adjacent MWCNT clusters in their inter-lamellas amorphous phase [Figure 12(a)]. Due to the limitation of space, the arrangement of MWCNT clusters would undergo some changes, discontiguous but neighboring clusters become connected by one or more MWCNT chains, so tiny MWCNT networks come into being inside β spherulites. Some MWCNT clusters can be involved in two distinct β spherulites for the large aspect ratio of MWCNT or MWCNT clusters, which act as a tie linking two β spherulites, as exhibited in Figure 12(b) and Figure 14(c). Accordingly, large conductive network comes into being, which is advantageous for improving the conductivity of samples. Besides, some clusters which are relatively far from β-NA would act as nucleation sites for inducing crystallization of α spherulites themselves, which have a compete growth with β-NA induced β crystals (Figure 6).

CONCLUSION

In order to explore the influence of β-NA on the morphology and properties of MWCNT-filled iPP. PLM and SEM observations, DSC and TGA tests, dynamic rheology, and conductivity properties measurements, notched impact strength tests were investigated in details in this study,

The incorporation of β-NA has promoted the dispersion of MWCNT in the iPP matrix, which is profitable for improving the thermal stability and conductivity properties of MWCNT-iPP composites. Besides, the 0.05 wt % β-NA nucleated samples exhibit higher impact toughness than that of un-β-NA-nucleated ones for relative high contents of β spherulites. The SEM observations show that the morphology of MWCNT changes from large agglomerations to small clusters with the doping of β-NA. The main reason is that the incorporation of β-NA (TMB-5) in MWCNT filled iPP matrix has led to the formation of a charge-transfer complex. Some of these clusters act as nucleation sites for crystallization of α spherulites, which have a compete growth with β-NA induced β crystals. Thus, the addition of MWCNT has decreased the relative contents of β-NA nucleated samples. Meanwhile, other clusters exist in the inter-lamella amorphous phase of β crystals, some of them even combine two adjacent β spherulites, thus a large conductive network comes into being.

Based on the investigated results, a model for explaining the mechanism concerning conductivity improvement by the incorporation of β-NA in MWCNT-filled samples is proposed.

ACKNOWLEDGMENTS

We would like to express our great thanks to National Natural Science Foundation of China (51010004) and State Key Laboratory of Molecular Engineering of Polymers (Fudan University) for financial support.

REFERENCES

1. Iijima, S. *Nature* **1991**, *354*, 56.
2. Ajayan, P. M.; Stephan, O.; Colliex, C.; Trauth, D. *Science* **1994**, *265*, 1212.
3. Codek, M.; Cohen, R. E. *Appl. Phys. Lett.* **2002**, *81*, 5123.
4. Long, Y.; Chen, Z. *Appl. Phys. Lett.* **2004**, *85*, 1796.
5. Xiao, K. Q.; Zhang, L. C.; Zarudi, I. *Compos. Sci. Technol.* **2007**, *67*, 177.
6. Yang, L. B.; Liu, F. H.; Xia, H. S.; Qian, X. Y.; Shen, K. Z.; Zhang, J. *Carbon* **2011**, *49*, 3274.
7. Dondero, W. E.; Gorga, R. E. *J. Polym. Sci. Polym. Phys.* **2006**, *44*, 864.

8. Mohammad, M.; Karen, I. W. *Macromolecules* **2006**, *39*, 5194.
9. Ke, K.; Wang, Y.; Zhang, K.; Luo, Y.; Yang, W.; Xie, B. H.; Yang, M. B. *J. Appl. Polym. Sci.* **2012**, *125*, 49.
10. Esawi, A. M. K.; Morsi, K.; Sayed, A; Taher, M.; Lanka, S. *Comp. Part A: Appl. Sci. Manufac.* **2011**, *42*, 234.
11. Chen, J.; Hamon, M. A.; Hu, H.; Chen, Y.; Rao, A. M.; Eklund, P. C.; Haddon, R. C. *Science* **1998**, *282*, 95.
12. Mitchell, C. A.; Bahr, J. L.; Arepall, S.; Tour, J. M.; Kishnammooti, R. *Macromolecules* **2002**, *35*, 8825.
13. Bubert, H.; Haiber, S.; Brandi, W.; Marginean; Heintze, M.; Bruser, V. *Diamond Relat. Mater.* **2003**, *12*, 811.
14. Eitan, A.; Jiang, K.; Dukes, D.; Andrews, R.; Schadler, L. S. *Chem. Mater.* **2003**, *15*, 3198.
15. Jang, J.; Bae, J.; Yoon, S. H. *J. Mater. Chem.* **2003**, *13*, 676.
16. Shaffer, M. S. P; Fan, X.; Windle, A. H. *Carbon* **1998**, *36*, 1603.
17. Star, A.; Stoddart, J. F.; Steuerman, D.; Diehl, M.; Boukai, A.; Wong, E. W.; Yang, X.; Chung, S. W.; Choi, Y. *Heath J. R. Angew. Chem. Int. Ed.* **2001**, *40*, 1721.
18. Jia, Z.; Wang, Z.; Xu, C.; Liang, W. B.; Wu, D.; Zhu, S. *Mater. Sci. Eng. A* **1999**, *271*, 395.
19. Deng, J.; Ding, X.; Zhang, W.; Peng, Y.; Wang, J.; Long, X. *Eur. Polym. J.* **2002**, *38*, 2497.
20. Safadi, B.; Andrews, R.; Grulke, E. A. *J. Appl. Polm. Sci.* **2002**, *84*, 2660.
21. Qian, D.; Dickey, E. C.; Andrew, R.; Rantell, T. *Appl. Phys. Lett.* **2000**, *76*, 2868.
22. Yin, C. L.; Liu, Z. Y.; Yang, W.; Yang, M. B.; Feng, J. M. *Coll. Polym. Sci.* **2009**, *287*, 615.
23. Dror, Y.; Salalha, W; Khalfin, R. L.; Cohen, Y.; Yarin, A. L.; Zussman, E. *Langmuir* **2003**, *19*, 7012.
24. Gong, X.; Liu, J.; Baskaran, S.; Voise, R. D.; Young, J. S. *Chem. Mater.* **2000**, *12*, 1049.
25. Kotek, J.; Kelnar, I.; Baldrian, J.; Raab, M. *Eur. Polym. J.* **2004**, *40*, 679.
26. Bai, H. W.; Wang, Y.; Zhang, Z. J.; Han, L.; Li, Y. L.; Liu, L.; Zhou, Z. W.; Men, Y. F. *Macromolecules* **2009**, *42*, 6647.
27. Li, J. X.; Cheung, W. L. *Polymer* **1998**, *39*, 6935.
28. Thiebaud, F.; Gelin, J. C. *Int. J. Mater. Form* **2009**, *2*, 149.
29. Bhattacharyya, A. R.; Sreekumar, T. V.; Liu, T.; Kumar, S.; Ericson, L. M.; Hauge, R. H.; Smalley, R. E. *Polymer* **2003**, *44*, 2373.
30. Assouline, E.; Lusiger, A.; Barber, A. H.; Cooper, C. A.; Klein, E.; Wachtel, E.; Wagner, H. D. *J. Polym. Sci. Part B Polym. Phys.* **2003**, *41*, 520.
31. Seo, M. K.; Lee, J. R.; Park, S. *J. Mater. Sci. Eng. A* **2005**, *404*, 79.
32. Avila-Orta, C. A.; Medellin, F. J.; Davila, M. V.; Aguirre, Y. A.; Yoon, K.; Hsiao, B. S. *J. Appl. Polm. Sci.* **2007**, *106*, 2640.
33. Barus, S.; Zanetti, M.; Bracco, P.; Musso, S.; Chiodoni, A.; Tagliaferro, A. *Polym. Degrad. Stab.* **2010**, *95*, 756.
34. Abbasi, S.; Derdouri, A.; Carreau, P. *J. Polym. Eng. Sci.* **2011**, *51*, 992.
35. Guldi, D. M.; Rahman, G. M. A.; Zerbetto, F.; Prato, M. *Acc. Chem. Res.* **2005**, *38*, 871.
36. Liu, B.; Lee, J. Y. *J. Phys. Chem. B* **2005**, *109*, 23783.
37. Chen, R. J.; Zhang, Y. G.; Wang, D. W.; Dai, H. J. *J. Am. Chem. Soc.* **2001**, *123*, 3838.
38. Cardoso, P.; Silva, J.; Klostermanc, D.; Covas, J. A.; Hattum, F. W. J.; Simoes, R.; Lanceros-Mendez, S. *Compos. Sci. Technol.* **2012**, *72*, 243.